Traffic Flow on a Ring With a Single Autonomous Vehicle: An Interconnected Stability Perspective

Vittorio Giammarino, Simone Baldi, Paolo Frasca, Maria Laura Delle Monache

Traffic Flow on a Ring with a Single Autonomous Vehicle: an Interconnected Stability Perspective

Vittorio Giammarino*, Simone Baldi†, Paolo Frasca‡
and Maria Laura Delle Monache§

Abstract

In recent years, field experiments have been performed on ring roadways with human-driven vehicles or with a mix of human-driven and autonomous vehicles. While these experiments demonstrate the potential for controlling traffic flows by a small number of autonomous vehicles, the theoretical framework about such a possibility is to a large extent incomplete. Indeed, most work on mixed traffic focused on classical asymptotical stability notions, neglecting that human drivers are prone to the interconnected instability known in the literature as string instability. This work aims to enhance the existing theories to meet the questions raised by the field experiments. It starts from the observation that the standard notion of string stability on a ring roadway is too demanding for a mixed traffic scenario: therefore, a new interconnected stability definition, named weak ring stability, is proposed. This new interconnected stability notion, in combination with classical stability, is able to explain phenomena observed in field experiments and to highlight possibilities and limitations of traffic control via sparse autonomous vehicle. Furthermore, it allows designing AV controllers with improved string stability specifications, at the price of reducing the sparsity of the autonomous vehicles.

*V. Giammarino is with Division of Systems Engineering, Boston University, 15 St Marys St, Brookline, MA 02446, USA and was with Delft Center for Systems and Control, Delft University of Technology (TU Delft), 2628 CD Delft, The Netherlands vittoriogiammarino@gmail.com

†S. Baldi is with School of Mathematics, Southeast University, Nanjing, China, and with Delft Center of Systems and Control, TU Delft, 2628 CD Delft, The Netherlands s.baldi@tudelft.nl

‡P. Frasca is with Univ. Grenoble Alpes, CNRS, Inria, Grenoble INP, GIPSA-Lab, 38000 Grenoble, France paolo.frasca@gipsa-lab.fr

§M. L. Delle Monache is with Univ. Grenoble Alpes, Inria, CNRS, Grenoble INP, GIPSA-Lab, 38000 Grenoble, France ml.dellemonache@inria.fr

Keywords
String stability, control of traffic flow, stability of traffic, autonomous vehicle, ring roadway.

1 Introduction

Several experimental settings have reproduced spontaneous emergence of stop-and-go waves in traffic flow. The first experiment of this kind is due to Sugiyama et al. in [29], who conducted an experiment with twenty-two *Human-driven Vehicles* (HVs) on a single-lane ring roadway as an approximation for an infinite open road. This experiment demonstrates how human driving behavior can be responsible of triggering stop-and-go waves. Recent advances in automation have brought forward the idea of exploiting *Autonomous Vehicles* (AVs) to dissipate stop and go waves and control traffic [8,11,12,14,17,30]. In 2018, Stern et al. [27] demonstrated experimentally that a single autonomous vehicle is able to dampen stop-and-go waves in the ring setup of [29]. In this ring setup, which approximates an open road in which AVs are sparsely introduced, controlling the AV dynamics is sufficient to prevent and even dissipate stop-and-go-waves.

Despite this practical evidence of the possibility of controlling traffic flows via a limited number of autonomous vehicles, the theoretical analysis around these experiments is still not complete. In fact, research on the effects of AVs on traffic has mostly focused on classical asymptotical stability notions: that is, perturbations around the equilibrium flow should be disappear as time goes by [16]. These studies, in fact, neglect another type of instability known in literature as interconnected or *string instability*, which is often observed in multi-vehicle platoons [3, 7, 19, 30]: a flow is said string stable if the effect (e.g. energy or magnitude) of a disturbance acting on one vehicle is not amplified throughout the platoon interconnection. Even when the flow is stable in the classical asymptotic sense, a string unstable flow can amplify disturbances over transients as per effect of vehicle interaction. To the best of our knowledge, the only paper looking at a single-lane lane string stability for heterogeneous platoons is [33], whose authors study the linearized model presented in [31] and derive a numerical bound for the penetration rate of the AVs to stabilize traffic. In this work, we extend the existing theories and provide a theoretical framework for the aforementioned experiments by studying both classical and interconnected stability on the ring roadway. Our framework is based on Linear Time Invariant (LTI) systems theory: this choice is consistent with most analytic studies on the topic

of mixed traffic [6,10,32,33,35], relying on linearization of the nonlinear vehicle dynamics around the equilibrium flow. Furthermore, LTI systems allow us to work in the frequency domain, in which string stability lends itself to a natural characterization based on the ratio of two transfer functions. Nonlinear analysis methods have been considered in literature [21], which however do not give insight on the design of stabilizing AVs.

Our analysis starts from the observation that the standard notion of string stability on a ring roadway is too demanding for a mixed traffic scenario, since human drivers are prone to string instability (and this drawback also affects current ACC systems [15], [18]). A new definition, named *weak ring stability*, is therefore proposed (Section 2). Classical asymptotic stability and weak ring stability are analyzed, first for the homogeneous HVs case and then for the mixed HVs-AV scenario (Sections 3 and 4, respectively). For both scenarios, it is shown that recently proposed sufficient conditions for classical stability [5, 35] can be very conservative, while a necessary and sufficient condition for classical stability for a ring of homogeneous HVs is formulated. It is shown that the proposed weak ring stability notion, in combination with classical stability, can explain the oscillatory phenomena occurring in the field experiments of [27, 29]. The weak ring stability notion also completes the currently-known range of possibilities and limitations of traffic control via sparse autonomous vehicle [5]: most notably, it indicates how to design mixed traffic scenarios with improved string stability specifications (dampening any oscillation). Key to this development is studying the AV controller originally proposed in [6], which employs a Proportional Integral (PI) control with saturation: once its limitations are understood, we can propose a novel design that partly overcomes them. Indeed, string stability can be ensured at the price of reducing the sparsity of the autonomous vehicles (Section 5).

Summarizing, the contributions of this work are: (i) a necessary and sufficient condition for classical stability for a ring of homogeneous HVs (Theorem 1); (ii) a theoretical framework for classical and string stability of HVs and mixed HVs-AV traffic on ring roadways (Definition 4, Theorem 2); (iii) a novel design procedure for AVs with improved performance (Theorem 3); and (iv) a discussion of the experimental findings in the light of our theoretical developments (Section 6).

Notation: The following notation is used throughout the paper: $\mathbb{C}$, $\mathbb{R}$, $\mathbb{N}$ are the sets of complex, real and natural numbers, $||\cdot||_\infty$ is the H_∞-norm in systems theory, $O_{n\times m}$ is the $n \times m$ zero matrix, and I_n is the $n \times n$ identity matrix. The product of elements in a set $\{x_j : j = 1, \ldots, n\}$ is written as $\prod_{j=1}^{n} x_j$, where by convention the product is 1 if the set is empty, i.e.

$\prod_{j\in\emptyset} x_j = 1$.

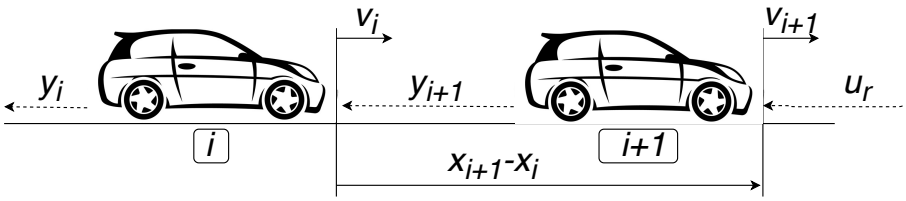

Figure 1: Scheme and notation for interconnected vehicles.

2 String stability definitions

In this section we provide the string stability definitions that are relevant to our work. We begin our presentation by recalling the relevant notions for vehicles on a line, before moving to our case of interest of the ring.

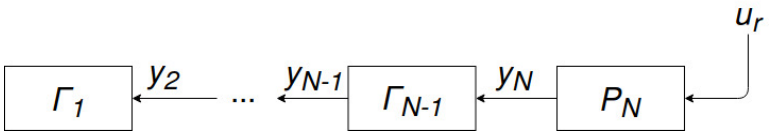

Figure 2: Block-diagram for interconnected vehicles on a line.

2.1 String Stability on the Line

Fig. 1 provides a graphical representation of the interaction between two adjacent vehicles in a predecessor-follower topology (also known as one-vehicle look-ahead interconnection). Let us recall some standard interconnected stability definitions with such a topology, noting that different topologies might require modified versions of the definitions stated in this section [7]. Let us assume for each vehicle i the linear *stable* vehicle model

$$y_i(s) = P_i(s)u_r(s), \quad s \in \mathbb{C} \tag{1}$$

where $y_i(s)$ and $u_r(s)$ are respectively the Laplace transforms of the vehicle output $y_i(t)$ and of the exogenous input $u_r(t)$ in Fig. 1. Typical outputs and inputs are velocities and acceleration commands, respectively, although different choices are also possible [23]: for example, $u_r(s)$ can also be seen

as an exogenous disturbance acting on the vehicles. From (1), it is possible to define

$$y_i(s) = \Gamma_i(s) y_{i+1}(s), \quad P_i(s) = \Gamma_i(s) P_{i+1}(s), \tag{2}$$

being $\Gamma_i(s)$ the transfer function between two adjacent vehicles outputs. A platoon is said to be "homogeneous" if all vehicles have identical dynamics in (2) ($\Gamma_i = \Gamma \ \forall i$), and "heterogeneous" otherwise. The interconnection of N possibly heterogeneous vehicles is given in Fig. 2 and leads to the transfer function:

$$y_i(s) = P_N(s) \prod_{j=i}^{N-1} \Gamma_j(s) u_r(s). \tag{3}$$

Based on (1)-(3), two notions of string stability on the line arise, named for brevity as *line stability*:

Definition 1 (Strong Line Stability (SLS) [23])**.** *Consider the linear line interconnected system whose input-output relation is described by (1) and* (2)*. Then, the system (3) is said to be* strong line stable *if*

$$||P_N(j\omega)||_\infty \quad \textit{is finite;} \tag{4}$$

$$||\Gamma_i(j\omega)||_\infty \leq 1 \quad \forall i \in \{1, \dots, N-1\}, \quad \forall N. \tag{5}$$

Definition 1 prevents amplification of the disturbance u_r between a vehicle i and its predecessor $i+1$ ($||P_i||_\infty = ||\Gamma_i P_{i+1}||_\infty \leq ||P_{i+1}||_\infty$). A weaker definition requires decreasing H_∞-norm on a fixed-length line, which does not exclude $||\Gamma_i||_\infty > 1$:

Definition 2 (Weak Line Stability (WLS))**.** *Consider the linear line interconnected system whose input-output relation is described by (1) and* (2)*. Then, the system (3) is said to be* weak line stable *if there exists a number N of vehicles such that*

$$||P_N(j\omega)||_\infty \quad \textit{is finite;} \tag{6}$$

$$||P_i(j\omega)||_\infty \leq ||P_{i+1}(j\omega)||_\infty \quad \forall i \in \{1, \dots, N-1\}. \tag{7}$$

From a physical point of view, the H_∞-norm represents the L_2 induced gain, i.e. the ratio between the energy of output and input signals [7], [23]. Both strong and weak string stability require decreasing the induced gain as per (7). However, Definition 1 asks (7) to hold for any arbitrary N (uniformity with respect to N), whereas Definition 2 asks (7) to hold for a fixed string length N: in fact, (7) can fail for too large N when $||\Gamma_i||_\infty > 1$

(lack of uniformity with respect to N). Different relaxations to Definition 1 have been studied in literature, such as the head-to-tail string stability [11]. In this work we consider a relaxation in the sense of Definition 2 motivated by analogous definitions for platoons on a ring, which are the object of the next subsection. These two notions motivate two analogous definitions for platoons on a ring, which are the object of the next subsection.

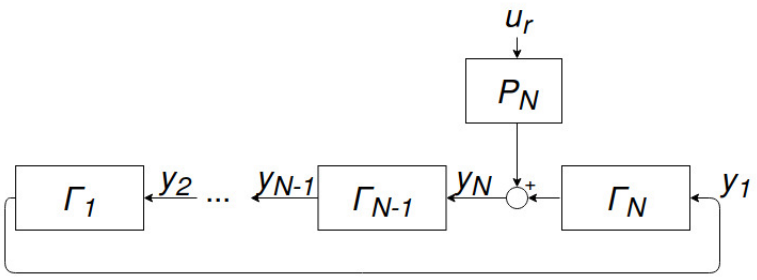

Figure 3: Block-diagram for interconnected vehicles on a ring.

2.2 String Stability on the Ring

The concept of string stability on a ring road topology is now considered, named for brevity as *ring stability*. The block diagram representation for N possibly heterogeneous vehicles on a ring is given in Fig. 3, and leads to the following transfer function:

$$y_i(s) = F_i^{(N)}(s)u_r(s), \quad F_i^{(N)}(s) = \Gamma_i(s)F_{i+1}^{(N)}(s), \tag{8}$$

$$F_i^{(N)}(s) = \frac{\prod_{j=i}^{N-1}\Gamma_j(s)}{1-\prod_{j=1}^{N}\Gamma_j(s)}P_N(s) \tag{9}$$

Even with the same number of vehicles N, ring and line present different structures, as the distribution of poles in the complex plane differs between (3) and (9). In (3), all poles are certainly in the left half-plane; the same does not hold in general for (9), as unstable poles might arise regardless of having stable poles in $P_i(s)$. Consequently, one cannot directly apply definitions given for a line: the notion of ring stability is less studied in literature and the most common one involves homogeneous platoons with $\Gamma_i = \Gamma$, $\forall i$ and

$$F_i^{(N)}(s) = \frac{\Gamma^{N-i}(s)}{1-\Gamma^N(s)}P_N(s). \tag{10}$$

Definition 3 (Strong Ring Stability (SRS) [22])**.** *Consider the linear homogeneous ring interconnection whose input-output relation is described by* (8) *(with* $\Gamma_i = \Gamma, \forall i$*). Further, assume* $||\Gamma||_\infty \leq 1$*. Then, the system (10) is said to be* strong ring stable *if there exists* $c > 0$ *such that*

$$||F_i^{(N)}(j\omega)||_\infty \leq c \quad i \in \{1, \dots, N\} \quad \forall N. \tag{11}$$

It is shown in [22] that SRS is equivalent to SLS for homogeneous platoons. Definition 3 is too restrictive in the applications, for several important reasons:

(a) It assumes $||\Gamma||_\infty \leq 1$ for all vehicles. Unfortunately, all human-driven vehicle models require $||\Gamma||_\infty > 1$ [10].

(b) It is based on homogeneity, i.e. it does not allow to consider a mixed traffic situation in which automated vehicles appear together with human-driven vehicles.

(c) Even though $||\Gamma||_\infty \leq 1$ is sufficient to ensure stability of (10), it is not necessary, since despite $||\Gamma||_\infty > 1$, $F_i^{(N)}(s)$ might have all its poles in the open-left-half plane. These cases are excluded by Definition 3.

These drawbacks make the definition unsuitable to be applied to Sugiyama's or Stern's experiments [27, 29]. To overcome these drawbacks, we propose a weaker notion of ring stability:

Definition 4 (Weak Ring Stability (WRS))**.** *Consider the linear possibly heterogeneous ring interconnection whose input-output relation is described by* (8)*. Then, for fixed* N*, system* (9) *is said to be* weakly ring stable *if*

$$||F_i^N(j\omega)||_\infty \quad \textit{is finite;} \tag{12}$$

$$||F_i^{(N)}(j\omega)||_\infty \leq ||F_{i+1}^{(N)}(j\omega)||_\infty \quad i \in \{1, \dots, N\}. \tag{13}$$

Remark 1 (*Benefits of WRS*)**.** Definition 4 implies that the effect of the worst-case disturbance is not amplified. Notably, as compared to Definition 3, we have that Definition 4:

(a) can address platoons of heterogeneous vehicles;

(b) does not require $||\Gamma_i||_\infty \leq 1$;

(c) covers the cases where (9) is stable although $||\Gamma_i||_\infty > 1$.

3 Traffic with Human Drivers

This section examines human-driven vehicles on a ring, by providing first their model and then classical stability and ring stability properties.

3.1 Human-driven Vehicle (HV) Model

The Optimal Velocity-Follow The Leader (OV-FTL) is a popular model for human driving behavior, taking the form

$$\begin{aligned} \dot{x}_i &= v_i \qquad i \in \{1, \dots, N\}, \\ \dot{v}_i &= \frac{v_{i+1} - v_i}{(x_{i+1} - x_i)^2} a + [V(x_{i+1} - x_i) - v_i] b \end{aligned} \tag{14}$$

where x_i is the position of vehicle i and v_i its velocity. Define $h_i = x_{i+1} - x_i$ as the headway, and note that $N + 1 = 1$, being the platoon on a ring. The nonlinear function $V(h_i)$ is

$$V(h_i) = \frac{\tanh(h_i - l_v - d_s) + \tanh(l_v + d_s)}{1 + \tanh(l_v + d_s)} v_{max} \tag{15}$$

being l_v the vehicle length and $d_s > 0$ a safety distance between vehicles; (15) determines the desired speed since it tends to zero for small h_i and approaches v_{max} for large h_i.
The parameters $a > 0$ and $b > 0$ in (14) represent weights between the OV and the FTL models [1, 2, 9].

Dynamics (14) has equilibrium

$$\begin{aligned} x_{i+1} - x_i &= h_* = \frac{l_r(N)}{N} \\ v_i &= v_{i+1} = v_* = V(h_*) \end{aligned} \tag{16}$$

where $l_r(N)$ is the circumference of the ring. Note that, in order to keep the same h_* when varying N, we vary l_r proportionally, that is why we write $l_r(N)$. Around this equilibrium the dynamics can be linearized as

$$\begin{aligned} \dot{x}_i &= v_i \qquad i \in \{1, \dots, N\} \quad (i = N + 1 = 1) \\ \dot{v}_i &= (v_{i+1} - v_i)\bar{a} + [(x_{i+1} - x_i)\bar{k} - \bar{c} - v_i]\bar{b} \end{aligned} \tag{17}$$

The linearization coefficients in (17) are calculated as:

$$\begin{aligned} \bar{k} &= \frac{\partial V(h_*)}{\partial h_i} = \frac{1 - \tanh^2(h_* - l_v - d_s)}{1 + \tanh(l_v + d_s)} v_{max}, \\ \bar{a} &= \frac{a}{h_*^2}, \quad \bar{b} = b, \quad \bar{c} = -\bar{k} h_* + V(h_*). \end{aligned} \tag{18}$$

The linearized model (17) broadly appears in traffic flow literature (cf. [10] and reference therein). In this literature it is common to consider a homogeneous human driving behavior: under such simplification, the HV dynamics in (17) result in the transfer function

$$\Gamma(s) = \frac{\bar{a}s + \bar{b}\bar{k}}{s^2 + (\bar{a} + \bar{b})s + \bar{b}\bar{k}} \tag{19}$$

derived by taking v_i as the output y_i in (2). It can be verified that the same transfer function is obtained using $y_i = v_i - v_{i-1}$. [23, 25].

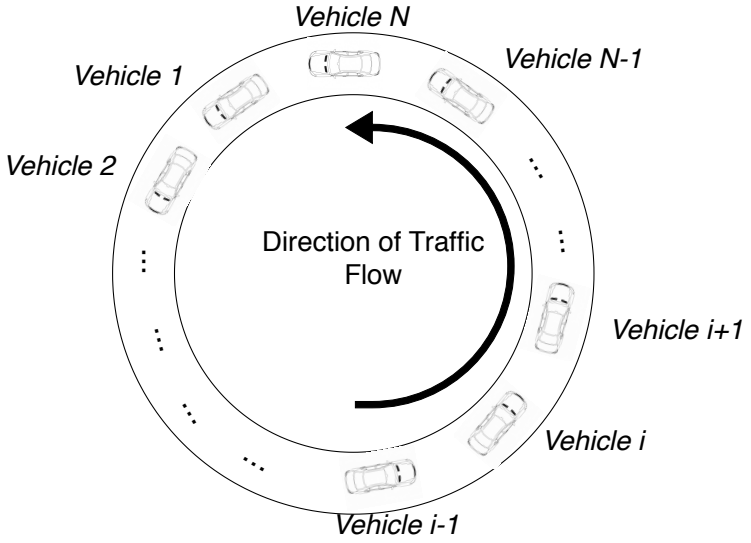

Figure 4: Schematic model of the ring road topology.

When put in a ring topology as in Fig. 4, the linearized OV-FTL model gives rise to a linear system which is the equivalent state-space formulation of (19):

$$\begin{bmatrix} \dot{\chi}_1 \\ \vdots \\ \dot{\chi}_{N-1} \\ \dot{\chi}_N \end{bmatrix} = \underbrace{\begin{bmatrix} A_1 & A_2 & O_{2\times 2} & \cdots & O_{2\times 2} \\ & \ddots & \ddots & & \\ O_{2\times 2} & \cdots & O_{2\times 2} & A_1 & A_2 \\ A_2 & O_{2\times 2} & \cdots & O_{2\times 2} & A_1 \end{bmatrix}}_{A} \begin{bmatrix} \chi_1 \\ \vdots \\ \chi_{N-1} \\ \chi_N \end{bmatrix} + \underbrace{\begin{bmatrix} 0 \\ \vdots \\ 0 \\ B_r \end{bmatrix}}_{B} u_r \tag{20}$$

where

$$A_1 = \begin{bmatrix} 0 & -1 \\ \bar{b}\bar{k} & -\bar{a} - \bar{b} \end{bmatrix} \quad A_2 = \begin{bmatrix} 0 & 1 \\ 0 & \bar{a} \end{bmatrix} \quad B_r = \begin{bmatrix} 0 \\ 1 \end{bmatrix}, \tag{21}$$

$\chi_i = \begin{bmatrix} x_{i+1} - x_i - h^*, & v_i - v^* \end{bmatrix}^T$ and where u_r in (20) represents an external disturbance, which is taken for convention acting on vehicle N.

3.2 Classical stability criteria

Before proceeding to the analysis of stability of (20) in the classical (asymptotic) sense, one observation is in order. As already observed in [35], the matrix A in (20) necessarily has one eigenvalue equal to 0 and its corresponding nontrivial eigenspace is spanned by the eigenvector $u = [1, \bar{k}, \ldots, 1, \bar{k}]^T$. This fact means that the dynamics of χ and the dynamics of $\chi + \alpha u$ coincide for any scalar α: note that replacing χ with $\chi + \alpha u$ would mean increasing all intervehicle distances and vehicle speeds by quantities whose ratio is $1/\bar{k}$. However, we are assuming the ring length to be fixed and therefore by definition $\sum_{i=1}^{N} \chi_i = [0, \sum_{i=1}^{N} v_i - N v^*]$: this constraint implies that the dynamics actually cannot evolve along the eigenvector u. For this reason, in our stability analysis we shall disregard the presence of this zero eigenvalue, similarly to what was done in [25, 28]: this choice is equivalent to removing the redundant states that arise from the ring structure by a suitable change of variable. To remind the reader that classical stability shall be established up to this structurally unavoidable zero eigenvalue, we shall say that matrix A is *structurally stable* when all its eigenvalues are negative, except the zero eigenvalue associated to u: also, whenever unambiguous, we will refer to this classical stability notion simply as stability. Note that literature conveniently assesses structural stability in the time domain via eigenvalue analysis of matrix A [5, 32, 35]; on the other hand, the different notions of string stability were conveniently studied in the frequency domain via transfer function analysis (cf. [23, 24] and [22, 25, 28] for line and ring configurations).

A sufficient condition for structural stability of (20)-(21) is known in literature.

Lemma 1 (Sufficient condition for stability [35])**.** *Consider the linear state-space system* (20) *arising from the ring interconnection of Fig. 4. Then, its equilibrium* (16) *is structurally stable if*

$$2\bar{a} + \bar{b} \geq 2\bar{k} \tag{22}$$

Table 1: Standard values used for the numerical analysis.

Variable name	Symbol	Value
Vehicle length	l_v	$4.5m$
Maximum vehicle velocity	v_{max}	$9.75m/s$
Safety distance	d_s	$6m$

Although (22) provides a simple analytical result to check stability of (20)-(21), it can be conservative, especially for relatively small N (conservativeness of (22) will be illustrated in Section 3.3). Therefore, we propose a necessary and sufficient condition which removes this conservativeness.

Theorem 1 (Necessary and sufficient condition for stability)**.** *Consider the linear state-space system* (20) *arising from the ring interconnection of Fig. 4. Then, its equilibrium* (16) *is structurally stable if and only if*

$$-\frac{1}{2}\gamma_i \pm \frac{1}{2}\left(\frac{\sqrt{r_i^2 + (\eta_i + 2\gamma_i\phi_i)^2} + r_i}{2}\right)^{1/2} \leq 0, \tag{23}$$

with

$$\gamma_i = \bar{a} + \bar{b} - \bar{a}\cos\left(\frac{2\pi(i-1)}{N}\right), \tag{24}$$

$$\phi_i = -\bar{a}\sin\left(\frac{2\pi(i-1)}{N}\right), \quad \eta_i = 4\bar{b}\bar{k}\sin\left(\frac{2\pi(i-1)}{N}\right), \tag{25}$$

$$r_i = \gamma_i^2 - \phi_i^2 - 4\bar{b}\bar{k}\left(1 - \cos\left(\frac{2\pi(i-1)}{N}\right)\right), \tag{26}$$

for all $i \in \{1, \ldots, N\}$ and the inequality is strict except for the structural zero eigenvalue that can be found by putting $i = 1$ and "+" in (23)*.*

Proof. See Appendix. □

3.3 Numerical analysis of stability

Let us investigate numerically the stability and WRS of (20)-(21) for different pairs (a, b) and by varying the number of vehicles N on the ring. The parameters in (15) are as in Tab. 1. In line with the experiment of Sugiyama, the headway equilibrium is taken as $h_* = 11.81m$, resulting in $\bar{k} = 1.2163$.

We begin by studying stability of (20)-(21) via Theorem 1 for different vehicle numbers N. In the (a,b)-plane, Fig. 5 illustrates that the stability region decreases by increasing N. The color-bar on the right-hand side associates colors with different numbers of vehicles N. For instance, the dark-blue area on the top-left is the instability region related to $N = 3$. Increasing to $N = 5$, an additional area (blue) turns unstable. Eventually, for $N \to \infty$ the instability region converges to the condition in (22) that is represented by a white line. The conservativeness of (22) arises from the fact that it is equivalent to $||\Gamma||_\infty \leq 1$ and therefore does not take into account the cases in which, despite $||\Gamma||_\infty > 1$, the equilibrium of (20) is in fact stable.

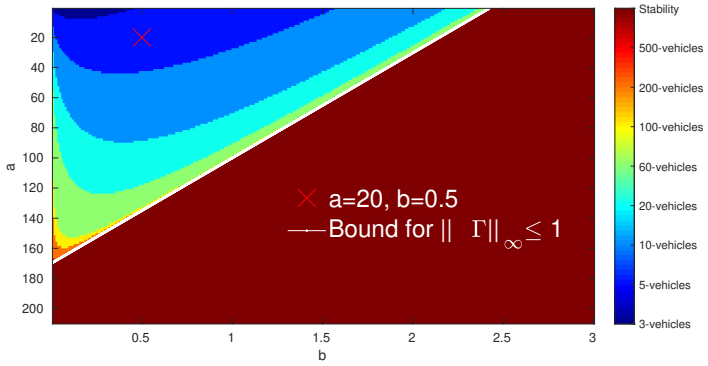

Figure 5: Stability of (20)-(21) in the (a,b)-plane, when changing N (c.f. color bar on the right). The stability region decreases when increasing N. For $N \to \infty$ the region tends to the sufficient condition (22), represented by a white line (the region above this line corresponds to $||\Gamma||_\infty > 1$).

Next, we proceed to fix some specific values of (a, b) and let N vary. Namely, we select

$$a = 20 \quad b = 0.5 \tag{27}$$

which have been proposed in literature for human drivers from field data [6, 27] and consider the two exemplary cases of $N = 3$ and $N = 22$. For $N = 3$, we can see that we have stability (cf. the $\times$ sign in Fig. 5). According to Definition 4, Fig. 6a shows that the peaks of $F_i^{(N)}(s)$ decrease while moving from vehicle 3, where the disturbance acts, to vehicle 1. Fig. 6b verifies the numerical analysis by simulating the nonlinear OV-FTL (14) with an impulse disturbance acting on vehicle 3 at $t = 60s$. The disturbance is not amplified between vehicles and its effect is rejected in about $40s$, indicating both stability and weak ring stability. Instead, for $N = 22$ as

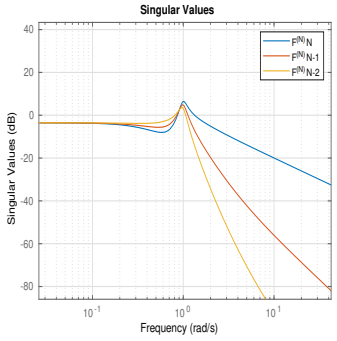

(a) Magnitudes of $F_i^{(N)}(s)$ $i \in \{1, 2, 3\}$.

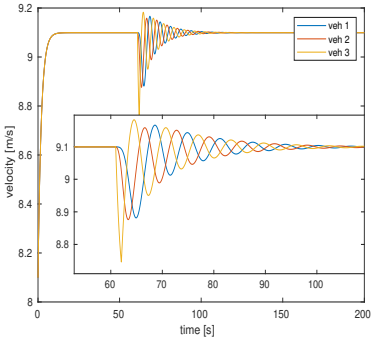

(b) Response to impulse disturbance at $t = 60s$.

Figure 6: WRS analysis and nonlinear simulation of the ring with $N = 3$, $a = 20$ and $b = 0.5$. An impulse disturbance at $t = 60s$ is not amplified denoting weak ring stability.

in Sugiyama's experiment, system (20)-(21) resulting from (27) is unstable. These evidences suggest that the wide oscillations seen in Sugiyama's experiment should be an outcome of the instability of the equilibrium, which consequently produces the onset of nonlinear oscillatory phenomena (Fig. 7 shows Sugiyama's experiment reproduced in simulations).

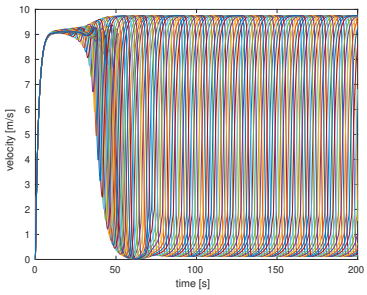

(a) Evolution of velocities over time.

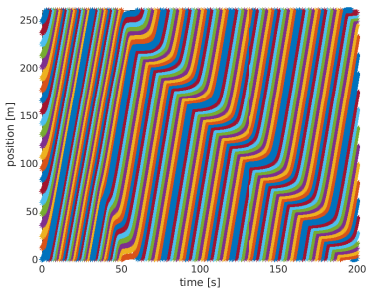

(b) Evolution of positions over time.

Figure 7: Nonlinear simulations with $N = 22$, $a = 20$ and $b = 0.5$, showing backward-travelling stop-and-go waves in line with Sugiyama's experiment.

4 Traffic with Single Autonomous Vehicle

This section studies a dynamics that describes the experiments in [27], where an AV is placed in the ring. We adopt the following convention: the AV is taken as the N-th vehicle, i.e. the AV follows vehicle 1 and precedes vehicle $N-1$. Consequently, we indicate with Γ_{AV} the transfer function from v_1 to v_N. Consider the following state-space formulation for the linearized platoon with $N-1$ HVs and a single AV:

$$\begin{bmatrix} \dot{\chi}_1 \\ \vdots \\ \dot{\chi}_{N-1} \\ \dot{\chi}_N \end{bmatrix} = \begin{bmatrix} A_1 & A_2 & & O_{2\times 2} \\ & \ddots & \ddots & \\ & & A_1 & A_2 \\ -A_{AV} & \dots & O & A_{AV} \end{bmatrix} \begin{bmatrix} \chi_1 \\ \vdots \\ \chi_{N-1} \\ \chi_N \end{bmatrix} + \begin{bmatrix} 0 \\ \vdots \\ 0 \\ B_r \end{bmatrix} u_r, \tag{28}$$

with A_1, A_2 and B_r as in (21) and $A_{AV} = [0 \quad 1; 0 \quad 0]$. The literature provides us with the following stabilizability result.

Lemma 2 (Stabilizability of mixed platoons [35])**.** *The linear state-space system in* (28) *is structurally stabilizable for all* $N \in \mathbb{N}$.

Lemma 2 states that it is *possible to stabilize any platoon of N vehicles by means of a single AV*, even though the stabilization of a large number of vehicles would incur performance limitations underlined in [5]. Since Lemma 2 is not a constructive result, it is important to have a criterion to verify whether a specific form of AV dynamics stabilizes the platoon. A sufficient condition for stability of a mixed HV-AV platoon is conjectured in [5], as an extension of the sufficient condition in Lemma 1. Such a conjecture is now proven:

Theorem 2 (Sufficient condition for stability of mixed platoons [5])**.** *Consider* $\Gamma(s)$ *as in* (19) *and* $\Gamma_{AV}(s)$ *the transfer function of the AV dynamics. The equilibrium of* (28) *is structurally stable if*

$$|\Gamma(j\omega)|^{1-\frac{1}{N}} \cdot |\Gamma_{AV}(j\omega)|^{\frac{1}{N}} \leq 1 \quad \omega \in \mathbb{R} \tag{29}$$

where $\frac{1}{N}$ *represents the ratio between HVs and AVs.*

Proof. See Appendix. □

Theorem 2 poses two natural questions.

- Since it was shown that the condition in Lemma 1 is conservative for HVs (cf. Fig. 5), it is interesting to see to what extent (29) is conservative for mixed platoons.
- Some AV designs have been proposed in the literature [6], and even used for the experiments in [27], but it is unclear if these designs meet condition (29).

Let us now address these two questions. We first focus on the AV controller, recalling AV designs in literature and proposing a novel design. Next, we investigate how conservative (29) is, showing that the condition is tight for large platoons.

4.1 Analysis of state-of-the-art AV control: PI with saturation

The starting point is the PI with saturation AV introduced in [6], whose nonlinear dynamics are

$$\begin{aligned} \dot{x}_N &= v_N \\ \dot{v}_N &= K_{veh}(\alpha v_{target} + (1-\alpha)v_1 - v_N) \end{aligned} \tag{30}$$

where v_{target} and α are defined via

$$\begin{aligned} v_{target} &= V_d + \min\Big(\max\Big(\frac{x_1 - x_N - 7}{\delta}, 0\Big), 1\Big) \\ V_d &= \Big(\frac{v_N + v_1}{2}\Big) \\ \Delta x_s &= \max\Big(2(v_1 - v_N), 4\Big) \\ \alpha &= \min\Big(\max\Big(\frac{x_1 - x_N - \Delta x_s}{\gamma}, 0\Big), 1\Big). \end{aligned} \tag{31}$$

As commonly considered in [36], $\delta > h_* - 7$, which leads to the following linearization

$$\begin{aligned} \dot{x}_N =& v_N \\ \dot{v}_N =& K_{veh}\Big((1-\alpha)v_1 + \alpha\frac{v_N + v_1}{2} + \alpha\frac{x_1 - x_N - 7}{\delta} - v_N\Big) \\ =& \frac{K_{veh}\alpha}{\delta}(x_1 - x_N) - K_{veh}\Big(1 - \frac{\alpha}{2}\Big)v_N \\ &+ K_{veh}\Big(1 - \frac{\alpha}{2}\Big)v_1 - 7\frac{K_{veh}\alpha}{\delta}. \end{aligned}$$

The corresponding transfer function is therefore

$$\Gamma_{AV}(s) = \frac{K_{veh}[(1-\frac{\alpha}{2})s + \frac{\alpha}{\delta}]}{s^2 + K_{veh}(1-\frac{\alpha}{2})s + K_{veh}\frac{\alpha}{\delta}}. \tag{32}$$

Using a condition similar to (22), it is possible to verify that $||\Gamma_{AV}||_\infty > 1$ for any choice of the parameters. Since in practice it happens that $||\Gamma||_\infty > 1$ for the HVs, we can conclude that, according to the linear criteria proposed in this work, the stabilizing AV in the experiments of [6] does meet weak ring stability criteria (we will further elaborate on our interpretation of the these experiments in Section V). In order to overcome this apparent lack of string stability, clearly it is preferable for the AV to have $||\Gamma_{AV}||_\infty \leq 1$, so as to damp the frequency peak of the HVs according to (13). Note from (32) that the AV is merely a second-order system with little degrees of freedom with respect to frequency shaping. In order to improve the overall platoon performance, it is therefore crucial to build on the previous analysis to improve the design in [6] and accomplish some form of ring stability.

4.2 Proposed AV control design

In view of the poor properties of AV dynamics (30), we propose the following improved design

$$\begin{aligned} \dot{x}_N &= v_N \\ \dot{v}_N &= K_{veh}(\alpha v_{target} + (1-\alpha)v_1 - v_N) + c(v_{AV*} - v_N) \end{aligned} \tag{33}$$

with variables as in (31), being v_{AV*} the desired velocity of the AV at equilibrium and $c > 0$ to be designed. Similarly to the previous design, $\delta > h^* - 7$ leads to the linearization

$$\begin{aligned} \dot{x}_N &= v_N \\ \dot{v}_N &= \frac{K_{veh}\alpha}{\delta}(x_1 - x_N) - \Big(K_{veh}\Big(1-\frac{\alpha}{2}\Big) + c\Big)v_N \\ &\quad + K_{veh}\Big(1-\frac{\alpha}{2}\Big)v_1 - \Big(\frac{7K_{veh}\alpha}{\delta} - cv_{AV*}\Big) \end{aligned} \tag{34}$$

and the following transfer function:

$$\Gamma_{AV}(s) = \frac{K_{veh}[(1-\frac{\alpha}{2})s + \frac{\alpha}{\delta}]}{s^2 + \Big(K_{veh}(1-\frac{\alpha}{2}) + c\Big)s + K_{veh}\frac{\alpha}{\delta}}. \tag{35}$$

It is not difficult to verify that $||\Gamma_{AV}||_\infty \leq 1$, provided that

$$\Big(K_{veh}\Big(1-\frac{\alpha}{2}\Big)+c\Big)^2 - K_{veh}^2\Big(1-\frac{\alpha}{2}\Big)^2 - 2K_{veh}\frac{\alpha}{\delta} \geq 0,$$

which is satisfied if c is large enough:

$$c > -K_{veh}\Big(1-\frac{\alpha}{2}\Big) + \sqrt{K_{veh}^2\Big(1-\frac{\alpha}{2}\Big)^2 + 2K_{veh}\frac{\alpha}{\delta}} \tag{36}$$

For this controller, the following stability result holds.

Theorem 3 (AV design for stability)**.** *Let us consider HVs as in* (19) *with (a,b) such that* $||\Gamma||_\infty > 1$ *and* Γ_{AV} *as in* (35)*. Then, condition* (29) *holds if* (36) *is satisfied and*

$$K_{veh} < \frac{\Big(1-\frac{\alpha}{2}\Big)c\bar{\omega}_\Gamma^2 - \frac{\alpha}{\delta}\bar{\omega}_\Gamma^2}{\Big[\frac{\alpha^2}{\delta^2} + \Big(1-\frac{\alpha}{2}\Big)^2\bar{\omega}_\Gamma^2\Big](||\Gamma||_\infty^{2(N-1)} - 1)} + \frac{\bar{\omega}_\Gamma\sqrt{\begin{array}{l} -\Big(1-\frac{\alpha}{2}\Big)^2\bar{\omega}_\Gamma^4 - \frac{\alpha}{\delta}\Big[2c\Big(1-\frac{\alpha}{2}\Big)\bar{\omega}_\Gamma^2 + \frac{\alpha}{\delta}c\Big] \\ +(\bar{\omega}_\Gamma^2 + c^2)\Big[\frac{\alpha^2}{\delta^2} + \Big(1-\frac{\alpha}{2}\Big)^2\bar{\omega}_\Gamma^2\Big]||\Gamma||_\infty^{2(N-1)} \end{array}}}{\Big[\frac{\alpha^2}{\delta^2} + \Big(1-\frac{\alpha}{2}\Big)^2\bar{\omega}_\Gamma^2\Big](||\Gamma||_\infty^{2(N-1)} - 1)} \tag{37}$$

where $\bar{\omega}_\Gamma = \arg\max_\omega |\Gamma(j\omega)|$.

Proof. See Appendix. □

It can be shown that the righthand side of (37) is strictly positive thanks to $||\Gamma||_\infty > 1$.

4.3 Conservativeness of the sufficient condition of stability

Here we investigate numerically the conservativeness of Theorem 2, resulting in condition (37). The numerical values used for the analysis are the same as in Tab. 1, with (a,b) in (27). Condition (37) is compared with the indirect Lyapunov method applied on the system

$$\begin{bmatrix} \dot{\chi}_1 \\ \vdots \\ \dot{\chi}_{N-1} \\ \dot{\chi}_N \end{bmatrix} = \begin{bmatrix} A_1 & A_2 & & O_{2\times 2} \\ & \ddots & \ddots & \\ & & A_1 & A_2 \\ A_{AV2} & \dots & 0 & A_{AV1} \end{bmatrix} \begin{bmatrix} \chi_1 \\ \vdots \\ \chi_{N-1} \\ \chi_N \end{bmatrix} + \begin{bmatrix} 0 \\ \vdots \\ 0 \\ B_r \end{bmatrix} u_r, \tag{38}$$

where A_1, A_2 and B_r are as in (21), and

$$A_{AV1} = \begin{bmatrix} 0 & -1 \\ \frac{\alpha K_{veh}}{\delta} & -\Big(K_{veh}(1-\frac{\alpha}{2})+c\Big) \end{bmatrix} \tag{39}$$

$$A_{AV2} = \begin{bmatrix} 0 & 1 \\ 0 & K_{veh}(1-\frac{\alpha}{2}) \end{bmatrix}. \tag{40}$$

System (38) represents the HVs with the linearized AV dynamics as N-th row, with design parameters $\delta = 23$, $\alpha = 0.9$, $c = 0.5$ for the AV. The numerical analysis in Fig. 8 shows that condition (37) is conservative for very small N, but works well for $N \geq 5$, which is the scope of interest of [27, 29].

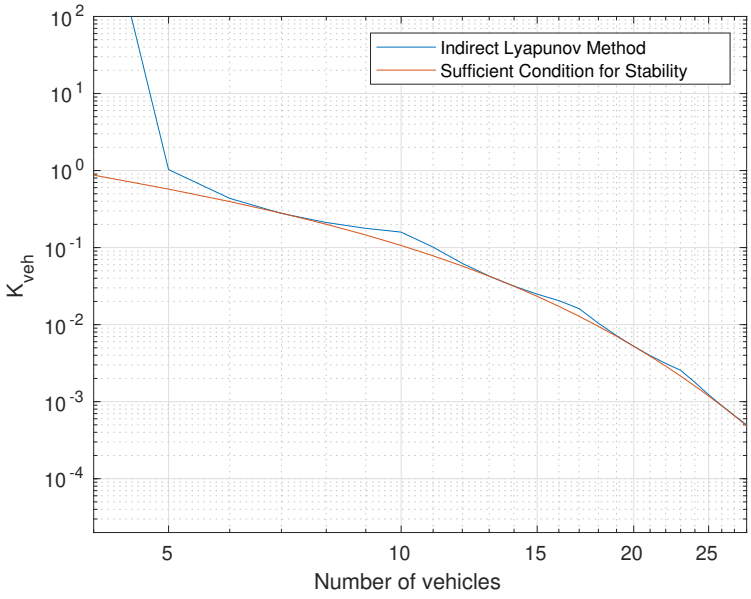

Figure 8: Comparison between the largest (structurally) stabilizing K_{veh} obtained from (37) and those obtained using the indirect Lyapunov method. For $N \leq 4$ the system is stable for any $K_{veh} > 0$.

5 Simulations on mixed HV-AV platoons

This section investigates the role of WRS (Definition 4) for mixed platoons with a single AV. Assuming an exogenous disturbance acting on the AV, the transfer function $F_i^{(N)}(s)$ for a vehicle i from disturbance to velocity is

$$F_i^{AV(N)}(s) = \frac{\Gamma^{N-i}(s)}{1 - \Gamma_{AV}(s)\Gamma^{N-1}(s)} P_N(s) \tag{41}$$

whose stability can be tested via Theorem 3. For $N = 22$, we find that a stabilizing gain is $K_{veh} = 0.0029$.

We simulate the ring with the stabilizing gain and the remaining parameters as in the previous section. Fig. 9a illustrates how the peak increases moving throughout the platoon denoting lack of weak ring stability according to Definition 4.

The lack of weak ring stability is confirmed by the nonlinear simulations. Fig. 9b shows that equilibrium is reached from zero initial conditions, indicating stability. However, a small $1s$ impulse disturbance on the AV ac-

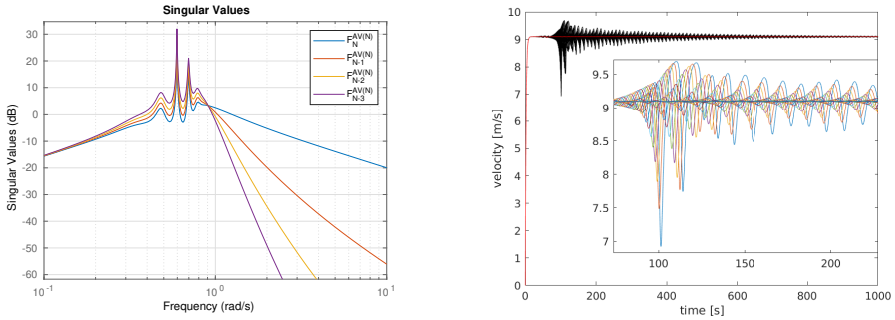

(a) Magnitudes of $F_i^{(N)}(s)$, $i = 19, 20, 21, 22$.

(b) Response to impulse disturbance at $t = 60s$.

Figure 9: WRS analysis and nonlinear simulations with $N = 22$ for a mixed traffic with modified AV (33). The peaks of $F_i^{(N)}(s)$ are amplified denoting ring instability. As a result, an impulse disturbance acting on the AV is amplified throughout the platoon.

celeration at t=60s creates a sizeable transient amplification throughout the platoon. This phenomenon poses the question of what happens if any additive noise (representing measurement noises or unmodelled dynamics) affects the platoon. The outcome is in Fig. 10a (where noise only affects the (N-1)-th HV) and in Fig. 10b (where noise affects all HVs). In both cases, noise

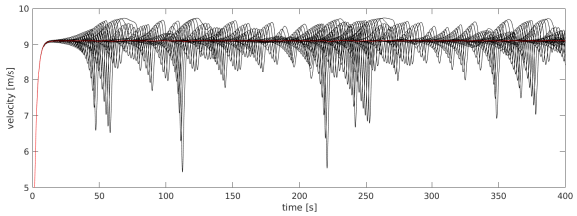

(a) Response to white noise on only the (N-1)-th HV with $15dB$ signal-noise-ratio

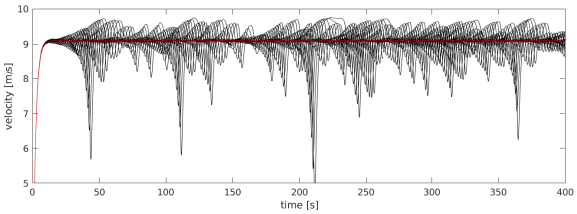

(b) Response to white noise on all the HVs with $20dB$ signal-noise-ratio.

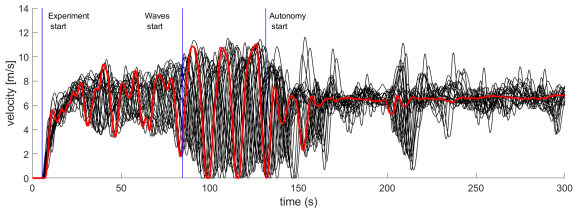

(c) Vehicles velocities measured during the experiment [27].

Figure 10: For the mixed traffic scenario of Fig. 9, the effect of a white noise on a single HV (Fig. 10a) is persistently amplified due to lack of weak ring stability. Similar effects occur when noises affect all HVs (Fig. 10b). This situation can be compared with experimental results of [8] (Fig. 10c). Vehicle velocities of [27] have been reproduced using the open source codes and data provided by the authors in [26]): our simulations qualitatively replicate the dynamics in the Autonomy phase after 150s.

creates oscillations that persistently appear and disappear. Indeed, Fig. 10b qualitatively replicates the behavior observed in the experiment [27] (cf. Fig. 3 in [27], reproduced in this work as Fig. 10c by using the open source code and data provided in [26]). Despite the different equilibrium velocities of the two flows, which are due to the different AV settings used in simulations and in field experiments, Fig. 10b is similar to the Autonomy phase

of Fig. 10c, where oscillations experience transient amplification. In conclusion, our simulations qualitatively replicate the dynamics in the Autonomy phase in [27], and show that AVs (34) cannot achieve both stability and ring stability when too sparse (1 AV out of 22 vehicles).

Ring stability becomes possible, instead, if the sparsity of AVs is reduced. For $N = 4$, the indirect Lyapunov method shows that (38) is stable for any $K_{veh} > 0$ (Fig. 8). We find that $K_{veh} = 15$ results in a decrease in the peaks of (41) according to Definition 4, which denotes weak ring stability (cf. Fig. 11a). Fig. 11b shows that a stable system that is also weak ring stable has a remarkably good response even with additive noise. In other words, the proposed WRS analysis explains how to design mixed traffic scenarios with improved string stability specifications (Fig. 10b vs Fig. 11b): the price to be paid is reducing the sparsity of the autonomous vehicles.

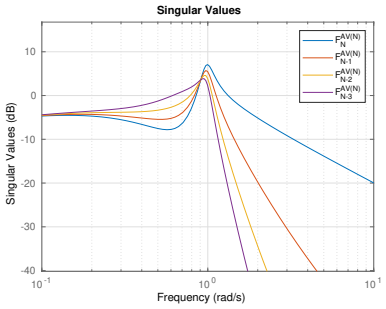

(a) Magnitudes of $F_i^{(N)}(s)$ $i \in \{1, 2, 3, 4\}$.

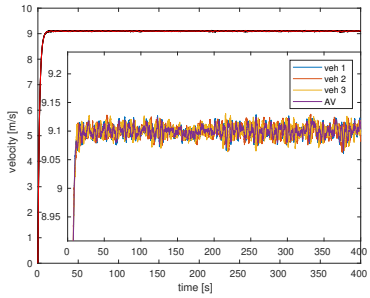

(b) Response to white noise with $20dB$ signal-noise-ratio.

Figure 11: WRS analysis and nonlinear simulation with $N = 4$ for a mixed traffic with modified AV (33). The peaks of $F_i^{(N)}(s)$ are not amplified denoting weak ring stability. Differently from Fig. 10b, when white noise is added to all the HVs, its effect is rejected throughout the platoon.

6 Stability in Sugiyama's and Stern's experiments

This concluding section aims to summarize what our system-theoretic framework tells us about the experiments in [29] and [27] and more generally about stabilizing traffic by AVs.

Sugiyama's experiment [29] has reproduced the spontaneous emergence of stop-and-go waves. Our study of the corresponding linearized dynamics shows that the dynamics is unstable, triggering the onset of large periodic

oscillations in the nonlinear dynamics. These theoretical findings and simulations, illustrated in Section 3, are consistent with the experimental evidence of stop-and-go waves. In Stern's experiment, the presence of an AV prevents and dampen stop-and-go waves. In Section 4, our study of the corresponding linearized dynamics has shown that the dynamics is (asymptotically) stable, but not string stable. Therefore, noise induces oscillations that are amplified only transiently, so that stop-and-go behavior is not triggered. Our theoretical findings and simulations are again consistent with the experiments that show a lack of stop-and-go waves but the presence of smaller, irregular, oscillations.

In order to guarantee better platooning performance, we have designed an improved AV controller that is able to ensure both stability and string stability for platoons with $N \leq 4$ vehicles. This ability has been theoretically verified and validated by simulations. Our analysis suggests that string stability can be achieved in platoons with HVs and AV, provided the ratio HV/AV is large enough. In fact, in contrast with the experiment in [27] where only $1/22 = 4.5\%$ of the vehicles is controlled (but string stability is not ensured), our result requires at least $1/4 = 25\%$ of the vehicles to be controlled to ensure string stability (compare Fig. 10b with Fig. 11b). It remains an open question whether better controllers can deliver string stability with fewer autonomous vehicles. Another open question is how to use communication among vehicles to improve string stability without increasing the number of AVs [8, 34].

A Proof of Theorem 1

For the sake of brevity we define $\alpha_1 = \bar{b}\bar{k}$, $\alpha_2 = \bar{a} + \bar{b}$, $\alpha_3 = \bar{a}$. Being (20) a block circulant matrix [20], an expression for its eigenvalues can be found as the eigenvalues of

$$\Lambda_i = A_1 + w^{i-1} A_2 = \begin{bmatrix} 0 & w^{(i-1)} - 1 \\ \alpha_1 & -\alpha_2 + w^{(i-1)}\alpha_3 \end{bmatrix},$$

$$\Lambda_i - \lambda I_2 = \begin{bmatrix} -\lambda & 1 \\ \alpha_1(w^{(i-1)} - 1) & -\alpha_2 + w^{(i-1)}\alpha_3 - \lambda \end{bmatrix},$$

$$\lambda^2 + (\alpha_2 - \alpha_3 \cdot w^{(i-1)})\lambda - \alpha_1(w^{(i-1)} - 1) = 0,$$

with $w = \exp(2\pi j/N)$ and $i \in \{1, \ldots, N\}$. The eigenvalues of Λ_i are

$$\begin{aligned}\lambda_{i,\pm} = &\frac{-\alpha_2 + \alpha_3 w^{(i-1)}}{2} \\ &\pm \frac{1}{2}\Big((\alpha_2 - \alpha_3 w^{(i-1)})^2 + 4\alpha_1(w^{(i-1)} - 1)\Big)^{1/2}.\end{aligned} \tag{42}$$

To ensure asymptotical stability we require that:

$$\begin{aligned}&Re\frac{-\alpha_2 + \alpha_3 w^{(i-1)}}{2} \pm \\ &Re\frac{1}{2}\Big((\alpha_2 - \alpha_3 w^{(i-1)})^2 + 4\alpha_1(w^{(i-1)} - 1)\Big)^{1/2} \leq 0,\end{aligned}$$

which is equivalent to (23).

B Proof of Theorem 2

The poles of a mixed platoon with a ring interconnection are given by the roots (λ) of

$$1 - \Gamma_{AV}(\lambda)\Gamma^{N-1}(\lambda) = 0 \tag{43}$$

where $\lambda = \mu + j\xi$. For all N, it can be shown that all the roots of (43) lie in the following subset of the complex plane:

$$\mathcal{C} = \{\lambda \in \mathbb{C} \quad : \quad |\Gamma(\lambda)|^{1-\gamma}|\Gamma_{AV}(\lambda)|^{\gamma} = 1\}, \tag{44}$$

where we defined as $\gamma = 1/N$ the ratio between the single AV and all vehicles. Function $|\Gamma(\lambda)|^{1-\gamma}|\Gamma_{AV}(\lambda)|^{\gamma}$ is a meromorphic function, which means that, given an open subset D of the complex plane, the function is holomorphic on all D except for the poles of the functions [4]. By definition, both Γ and Γ_{AV} have the poles in the open left half plane, indicating that $|\Gamma(\lambda)|^{1-\gamma}|\Gamma_{AV}(\lambda)|^{\gamma}$ is holomorphic in the closed right half plane. That is: the function is complex differentiable at every point of the considered subset and its maximum value lies along the edge of its domain. Being the domain the closed right half plane, its edge is the imaginary axis [4]. Consequently, ensuring $|\Gamma(j\xi)|^{1-\gamma}|\Gamma_{AV}(j\xi)|^{\gamma} \leq 1$ for all $\xi \in \mathbb{R}$ we can ensure that does not exist any $\lambda = \mu + j\xi$ with $\mu > 0$ such that $|\Gamma(j\xi)|^{1-\gamma}|\Gamma_{AV}(j\xi)|^{\gamma} = 1$. In other words, we ensure that there does not exist any $\lambda \in \mathbb{C}$ which is at the same time root of (43) and has strictly positive real part.

C Proof of Theorem 3

The most critical point for condition (29) is given by $||\Gamma||_\infty$, the peak of (19). This peak occurs at frequency $\bar{\omega}_\Gamma$. Thus, condition (29) leads to the following inequality

$$\left(\frac{K_{veh}^2[(1-\frac{\alpha}{2})^2\bar{\omega}_\Gamma^2 + \frac{\alpha^2}{\delta^2}]}{(\frac{K_{veh}\alpha}{\delta} - \bar{\omega}_\Gamma^2)^2 + \bar{\omega}_\Gamma^2[K_{veh}(1-\frac{\alpha}{2}) + c]^2} \right) ||\Gamma||_\infty^{2(N-1)} < 1 \tag{45}$$

By developing (45), the following inequality is obtained

$$\begin{aligned} &K_{veh}^2 \left[\frac{\alpha^2}{\delta^2} + \left(1 - \frac{\alpha}{2}\right)^2 \bar{\omega}_\Gamma^2 \right] (||\Gamma||_\infty^{2(N-1)} - 1) \\ &+ 2K_{veh} \left(\frac{\alpha}{\delta}\bar{\omega}_\Gamma - \left(1 - \frac{\alpha}{2}\right) c\bar{\omega}_\Gamma^2 \right) - (\bar{\omega}_\Gamma^4 + \bar{\omega}_\Gamma^2 c) < 0 \end{aligned} \tag{46}$$

which yields (37).

Acknowledgements

This work was initiated by a Descartes Fellowship by the French Embassy in the Netherlands under project AMAS. S. Baldi was supported by the Fundamental Research Funds for the Central Universities grant no.4007019109 (RECON-STRUCT), and by the special guiding funds for "double first-class" grant no.4007019201. M.L. Delle Monache was supported by the IDEX-IRS 2018 project "MAVIT - Modeling autonomous vehicles in traffic flow". P. Frasca was partly supported by ANR via project HANDY, number ANR-18-CE40-0010. The authors are grateful to mr. Maolong Lv for some preliminary HVs simulations that were included in an early and incomplete account of this research [13].

References

[1] M. Bando, K. Hasebe, K. Nakanishi, and A. Nakayama. Analysis of optimal velocity model with explicit delay. *Physical Review E*, 58(5):5429, 1998.

[2] M. Bando, K. Hasebe, A. Nakayama, A. Shibata, and Y. Sugiyama. Dynamical model of traffic congestion and numerical simulation. *Physical Review E*, 51(2):1035, 1995.

[3] B. Besselink and K. H. Johansson. String stability and a delay-based spacing policy for vehicle platoons subject to disturbances. *IEEE Transactions on Automatic Control*, 62(9):4376–4391, 2017.

[4] R. B. Burckel. *An introduction to classical complex analysis*, volume 1. Academic Press, 1980.

[5] S. Cui, B. Seibold, R. Stern, and D. B. Work. Stabilizing traffic flow via a single autonomous vehicle: Possibilities and limitations. In *2017 IEEE Intelligent Vehicles Symposium (IV)*, pages 1336–1341. IEEE, 2017.

[6] M. L. Delle Monache, T. Liard, A. Rat, R. E. Stern, R. Badhani, B. Seibold, J. Sprinkle, D. B. Work, and B. Piccoli. Feedback control algorithms for the dissipation of traffic waves with autonomous vehicles. In *Computational Intelligence and Optimization Methods for Control Engineering*, pages 275–299. Springer, 2019.

[7] S. Feng, Y. Zhang, S. E. Li, Z. Cao, H. X. Liu, and L. Li. String stability for vehicular platoon control: Definitions and analysis methods. *Annual Reviews in Control*, 47:81–97, 2019.

[8] A. Firooznia, J. Ploeg, N. van de Wouw, and H. Zwart. Co-design of controller and communication topology for vehicular platooning. *IEEE Transactions on Intelligent Transportation Systems*, 18(10):2728–2739, 2017.

[9] D. C. Gazis, R. Herman, and R. W. Rothery. Nonlinear follow-the-leader models of traffic flow. *Operations research*, 9(4):545–567, 1961.

[10] J. Ge. *Connected Cruise Control Design in Mixed Traffic Flow Consisting of Human-Driven and Automated Vehicles*. PhD thesis, University of Michigan, 2017.

[11] J. Ge and G. Orosz. Dynamics of connected vehicle systems with delayed acceleration feedback. *Transportation Research Part C: Emerging Technologies*, 46:46–64, 2014.

[12] J. I. Ge and G. Orosz. Optimal control of connected vehicle systems with communication delay and driver reaction time. *IEEE Transactions on Intelligent Transportation Systems*, 18(8):2056–2070, 2017.

[13] V. Giammarino, M. Lv, S. Baldi, P. Frasca, and M. Delle Monache. On a weaker notion of ring stability for mixed traffic with human-driven and autonomous vehicles. In *IEEE Conference on Decision and Control*, pages 335–340, Nice, France, Dec. 2019.

[14] S. Gong and L. Du. Cooperative platoon control for a mixed traffic flow including human drive vehicles and connected and autonomous vehicles. *Transportation Research Part B: Methodological*, 116:25–61, 2018.

[15] G. Gunter, D. Gloudemans, R. E. Stern, S. McQuade, R. Bhadani, M. Bunting, M. L. Delle Monache, R. Lysecky, B. Seibold, J. Sprinkle, et al. Are commercially implemented adaptive cruise control systems string stable? *arXiv preprint arXiv:1905.02108*, 2019.

[16] H. K. Khalil and J. W. Grizzle. *Nonlinear systems*, volume 3. Prentice hall Upper Saddle River, NJ, 2002.

[17] S. Knorn, A. Donaire, J. C. Agüero, and R. H. Middleton. Passivity-based control for multi-vehicle systems subject to string constraints. *Automatica*, 50(12):3224–3230, 2014.

[18] M. Makridis, K. Mattas, and B. Ciuffo. Response time and time headway of an adaptive cruise control. an empirical characterization and potential impacts on road capacity. *IEEE Transactions on Intelligent Transportation Systems*, 21(4):1677–1686, 2019.

[19] R. H. Middleton and J. H. Braslavsky. String instability in classes of linear time invariant formation control with limited communication range. *IEEE Transactions on Automatic Control*, 55(7):1519–1530, 2010.

[20] B. J. Olson, S. W. Shaw, C. Shi, C. Pierre, and R. G. Parker. Circulant matrices and their application to vibration analysis. *Applied Mechanics Reviews*, 66(4):040803, 2014.

[21] G. Orosz, R. E. Wilson, and G. Stépán. Traffic jams: dynamics and control. *Philosophical Transactions of the Royal Society. Series A.*, 368(1928):4455, 2010.

[22] A. A. Peters, R. H. Middleton, and O. Mason. Cyclic interconnection for formation control of 1-d vehicle strings. *European Journal of Control*, 27:36–44, 2016.

[23] J. Ploeg, N. Van De Wouw, and H. Nijmeijer. l_p string stability of cascaded systems: Application to vehicle platooning. *IEEE Transactions on Control Systems Technology*, 22(2):786–793, 2014.

[24] G. Rödönyi. Heterogeneous string stability of unidirectionally interconnected mimo lti systems. *Automatica*, 103:354–362, 2019.

[25] J. A. Rogge and D. Aeyels. Vehicle platoons through ring coupling. *IEEE Transactions on Automatic Control*, 53(6):1370–1377, 2008.

[26] R. E. Stern, S. Cui, M. L. Delle Monache, R. Bhadani, M. Bunting, M. Churchill, N. Hamilton, H. Haulcy, R'mani Pohlmann, F. Wu, B. Piccoli, B. Seibold, J. Sprinkle, and D. Work. Dissipation of stop-and-go waves via control of autonomous vehicles: Experimental results: Data. `http://hdl.handle.net/1803/8766`, 2018.

[27] R. E. Stern, S. Cui, M. L. Delle Monache, R. Bhadani, M. Bunting, M. Churchill, N. Hamilton, H. Pohlmann, F. Wu, B. Piccoli, B. Seibold, J. Sprinkle, and D. B. Work. Dissipation of stop-and-go waves via control of autonomous vehicles: Field experiments. *Transportation Research Part C: Emerging Technologies*, 89:205–221, 2018.

[28] S. Stüdli, M. M. Seron, and R. H. Middleton. Vehicular platoons in cyclic interconnections. *Automatica*, 94:283–293, 2018.

[29] Y. Sugiyama, M. Fukui, M. Kikuchi, K. Hasebe, A. Nakayama, K. Nishinari, S. Tadaki, and S. Yukawa. Traffic jams without bottlenecks experimental evidence for the physical mechanism of the formation of a jam. *New Journal of Physics*, 10(3):033001, 2008.

[30] D. Swaroop and K. J. Hedrick. String stability of interconnected systems. *IEEE Transactions on Automatic Control*, 41(3):349–357, 1996.

[31] M. Treiber, A. Hennecke, and D. Helbing. Congested traffic states in empirical observations and microscopic simulations. *Physical Review E*, 62(2):1805, 2000.

[32] J. Wang, Y. Zheng, Q. Xu, J. Wang, and K. Li. Controllability analysis and optimal controller synthesis of mixed traffic systems. In *2019 IEEE Intelligent Vehicles Symposium (IV)*, pages 1041–1047. IEEE, 2019.

[33] C. Wu, A. M. Bayen, and A. Mehta. Stabilizing Traffic with Autonomous Vehicles. In *IEEE International Conference on Robotics and Automation*, pages 6012–6018, 2018.

[34] L. Zhang and G. Orosz. Motif-based design for connected vehicle systems in presence of heterogeneous connectivity structures and time delays. *IEEE Transactions on Intelligent Transportation Systems*, 17(6):1638–1651, 2016.

[35] Y. Zheng, J. Wang, and K. Li. Smoothing traffic flow via control of autonomous vehicles. *arXiv preprint arXiv:1812.09544*, 2018.

[36] W.-X. Zhu and H. M. Zhang. Analysis of mixed traffic flow with human-driving and autonomous cars based on car-following model. *Physica A: Statistical Mechanics and its Applications*, 496:274–285, 2018.